JOURNAL OF MATERIALS SCIENCE 12 (1977) 708–717

The mechanism of reinforcement of polyurethane foam by high-modulus chopped fibres

T. C. COTGREAVE, J. B. SHORTALL
Department of Metallurgy and Materials Science, The University of Liverpool, Liverpool, UK

The morphology and fracture behaviour of polyurethane foams reinforced by short chopped fibres have been investigated. The presence of the fibres is shown to give rise to localized change in the foam morphology and the extent of this depends upon the fibre bundle size which is affected by the surface treatment. The changes in morphology are correlated with changes in the tensile properties of the foams at ambient and cryogenic temperatures. The systems are shown to be matrix limited with failure occurring remote from the interface which assumes a poassive role during tensile fracture. A critical fibre length for reinforcement of polyurethane foam, which depends on matrix shear strength and foam density, is defined.

1. Introduction

For many years the study of high-performance structural materials comprising high strength fibres combined with matrix materials of moderate strengths has been at the forefront of composites research. However, relatively little attention has been paid to the reinforcement of weaker matrices including foamed plastics, which are of interest because of their unique combination of properties such as low thermal conductivity, low density and high specific modulus. The use of foamed plastics for structural components allows the section thickness and hence the rigidity to be increased for a given weight of material.

Polyurethane foams are some of the most versatile of the foamed plastics systems available and their production has increased markedly in recent years. They can be fabricated in flexible, semi-flexible or rigid form by the reaction of a polyol and an isocyanate [1]. The type of foam produced is largely dependent on the molecular weight and hydroxyl content of the polyol, and it can be modified by the addition of cross-linking agents together with catalysts and surfactants. The density of the foam is controlled by the inclusion of one or more blowing agents, which may also be chemically reactive.

The structure of rigid polyurethane foam depends on the co-ordinated action of the catalysts, blowing agents and surfactants and, in a free-rise system, each cell will approximate to the theoretically predicted dodecahedral shape [2]. Some elongation of the cells will occur in the rise direction and mechanical restraints cause more pronounced deformation as the foam expands along the line of minimum local resistance.

Within the bounds of a particular foam formulation, the mechanical properties can be related to the foam density [3–5], whilst the cellular nature of the microstructure determines the mode of failure under stress [6, 7].

In order to improve the strength of polyurethane foam, milled glass fibres have been used as a filler [8–12] and short glass fibres have been incorporated into the resin struts [13]. The reinforcement of moulded and sprayed foams with longer chopped glass fibres and with continuous fibres has also been achieved, but in a largely empirical manner [14–19].

In a composite with a solid plastic matrix,

the surface treatment applied to the reinforcing agent is frequently a dominating factor in controlling the fracture processes. The degree of control that can be exercised over the interfacial bond strength permits a fibre/matrix combination to be optimized for a given purpose. There is, however, no information on the mechanism by which the incorporation of fibres reinforces a foam, or the way in which the fibres affect the microstructure. The objectives of this work, therefore, were to study the relationship between the structure of the reinforced foam and the ultimate strength properties and to determine the role of the interface in controlling the fracture processes. The effect of temperature on these properties has also been investigated.

2. Experimental

2.1. Materials

Rigid closed-cell foams were prepared from a "Caradol-Caradate" blend supplied by Shell Chemicals (UK) Limited, using trichlorofluoromethane as blowing agent. Two densities were used, one at 35 kg m^{-3} to provide a model system for a detailed study of fracture processes in the foam, and the other at 80 kg m^{-3} to evaluate the effects of the inclusion of glass fibres on the mechanical properties of the foam.

Chopped glass fibres were supplied by Pilkington Research Laboratories in 3, 6, 12 and 24 mm lengths with a nominal filament diameter of 13 μm. During the manufacturing process, one of two proprietary sizes was applied to the glass immediately after the fibres were drawn; one was classed as "polyurethane compatible" and the other as nominally "non-compatible". Following removal of the "non-compatible" size from fibres by heating to 500°C, one portion was allowed to adsorb atmospheric moisture and another was treated with PTFE preparations in an attempt to provide a chemically inert surface. However, since it was found impossible to achieve complete coverage of the filaments, the effect of an inert surface was investigated by analogy using 7 to 8 μm untreated Morganite Modmor Type 1 carbon fibres. Continuous rovings treated with the non-compatible size at two different concentrations (approximately 1% wt, which is the usual concentration, and 0.7% wt) were used in later experiments to prepare samples for mechanical testing.

2.2. Specimen preparation

A quantity of the heat-cleaned chopped fibres was mixed with the isocyanate component and thoroughly dispersed before the addition of the polyol blend. After curing, specimens of the foam were cut for microscopic examination and this confirmed that minimum distortion of the classical foam structure had been obtained. Only low concentrations of glass (<5 wt %) could be achieved by stirring the fibres into the foam reagents; the dramatic increase in viscosity with higher loadings inhibited efficient mixing. However, small samples of foam containing the treated fibres were prepared by a similar method which involved tamping the fibres into the prefoamed mixture in a polythene bag. The dispersion of glass was far from ideal, but a number of specimens containing suitably aligned fibres and fibre bundles were obtained, to permit the fracture properties to be studied.

The high-density foams were obtained by spraying and 12 mm fibres were incorporated by projecting them directly from a chopper fed with glass roving. Samples of these foams were cut to form dumbell-shaped tensile specimens 150 mm x 40 mm x 40 mm, waisted to 25 mm x 25 mm. Metal end plates were attached with Plastic Padding (Plastic Padding Ltd, High Wycombe, Bucks) before testing.

2.3. Microscopy

Specimens for microscopy were cut on a low speed "Isomet" diamond wafering saw running in 60-80 petroleum spirit; foam debris was removed by ultrasonic cleaning in isopentane. Microscopic examination of the specimens was carried out using a Reichert polarizing microscope and a Zeiss Tessovar photomicrographic system with an extended depth of field. A miniature tensioning jig was constructed which had a double-glazed perspex base to permit observation in transmitted light and to permit the fracture processes to be monitored under the microscope with the specimen immersed in liquid nitrogen. As a further aid to following the fracture sequences, the jig was mounted on its own illuminating source and recordings were made via a closed circuit television camera and monitor.

Specimens 60 mm x 15 mm and 1 to 2 mm thick were placed in the jig, and either a single

notch was cut with a scalpel or two notches were cut, one from either side, normal to the tensile axis and approaching a selected filament. For low temperature testing the jig was filled with liquid nitrogen before gradually applying a load to propagate the crack. In between each stage of crack extension the specimen could be relaxed by reducing the load to permit photography. Finally the specimen was loaded to complete failure and the fracture surfaces were examined.

2.4. Tensile tests

The faces of the dumbell shaped tensile specimens were cut parallel on a high speed diamond saw, the waist was cut with a band saw and finished on a belt sander. Tensile testing was carried out on an "Instron" machine at a cross-head speed of $10\,mm\,min^{-1}$ and an extensometer was used to facilitate modulus measurements. For low temperature work, an insulated container was fitted to the lower socket of the Instron and the test specimen was immersed in liquid nitrogen.

3. Results

3.1. Morphology

Microscopic examination of unfilled polyurethane foam revealed a well ordered structure of regularly shaped gas-filled cells bounded by solid resin struts and enclosed by resin windows. Fig. 1 shows the typical structure of a cell face in which the struts, intersections and windows are clearly defined.

The foams containing fibres that were free to rise as the foam expanded had not suffered any gross distortion of the bulk matrix structure; however, a number of more localized features

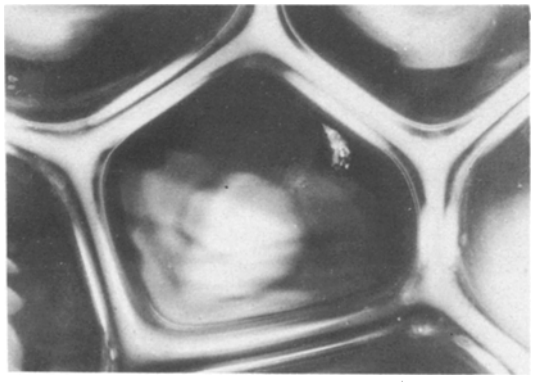

Figure 1 Typical structure of a cell face showing struts, intersections and window.

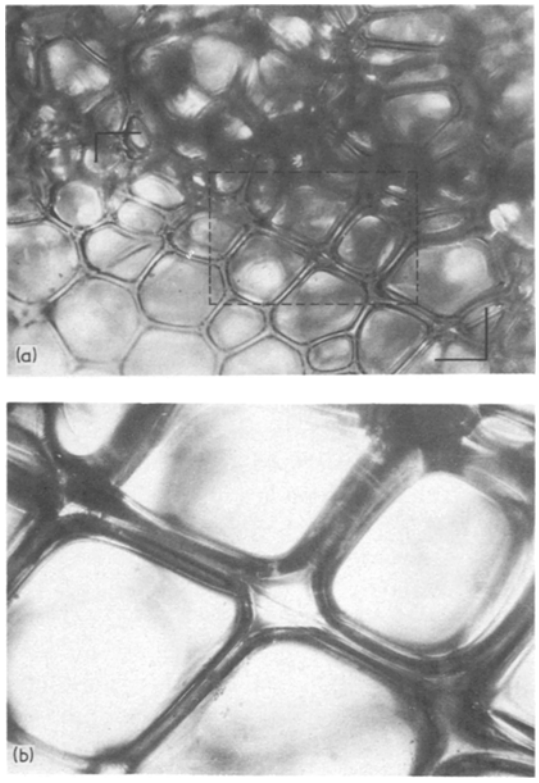

Figure 2 (a) An elongated composite strut formed from a single filament. (b) Enlargement of central section of (a) showing the filament within the sheath.

relating to fibre bundle size were revealed.

Large fibre bundles (of around 100 filaments or more) contained many inner members that were not attached to the foam. A thin layer of resin coated the outer members and the cells that developed on this were smaller than those in the bulk of the matrix.

Small fibre bundles (of about 10 filaments) were also encased by cells, but these were not reduced in size relative to the bulk, which reflects the effect of the lower heat capacity of the smaller mass of glass on the reaction exotherm.

The ultimate dispersion of a fibre bundle as single filaments created a situation in which each filament formed the core of an elongated composite strut with cells built up radially along its length as shown in Fig. 2a; Fig. 2b shows an enlargement of the central zone where the filament can be seen within the sheath. The cells were regular and comparable in size to those in the bulk of the matrix, and distortion was limited to the alignment of the cells on the common base afforded by the filament.

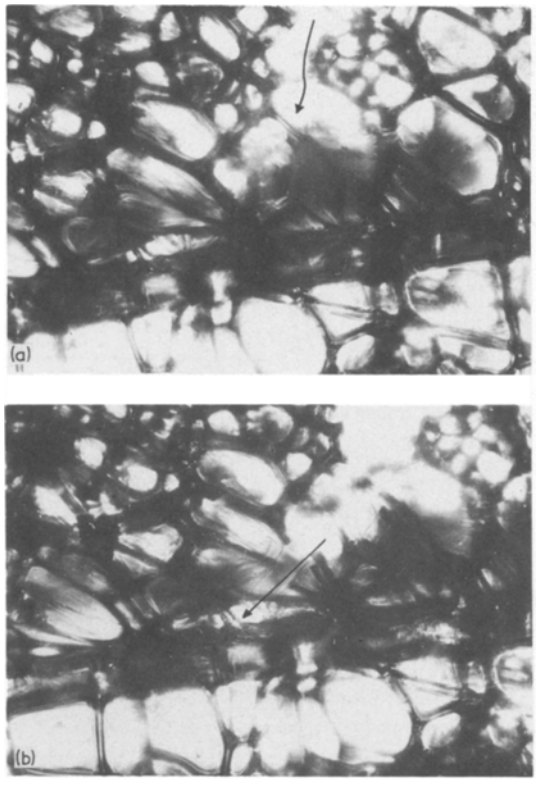

Figure 3 (a) Crack (arrowed) in foam matrix approaching small fibre bundle. (b) Start of crack deflection. (c) Progressive failure of radial struts.

3.2. Fracture behaviour

The miniature jig was used to follow crack propagation in the reinforced foams. The effects of the different fibre surface treatments and of bundle size and test temperature on the modes of failure of the model specimens were also studied.

Fig. 3 shows stages in the progression and diversion of a crack by a small bundle of glass in a specimen tensioned in the jig at room temperature. Fig. 3a shows the crack, which was started and directed towards the mid-point of the 12 mm bundle, and indicates where it was arrested until further load was applied. Fig. 3b shows the situation after increasing the load; the crack has moved nearer to the bundle and has started to divert parallel to it. The tip of the crack can be seen where it has passed through one of the cell windows and come to rest at a strut. Fig. 3c shows the failure of this strut and the subsequent failure of several neighbouring struts as the crack progressed towards the end of the bundle. This crack progression though all the remaining struts resulted in the formation of a "pull-out" fragment. The crack has not reached the interface and no debonding has occurred; the glass remaining encased in the resin sheath. Fig. 4 shows a pull-out fragment with a fibre encased in a resin sheath and surrounded by broken struts. This same mode of failure predominated for all small bundles irrespective of surface treatment or test temperature.

The larger bundles of fibres (inherent from the use of "compatible" size) gave rise to a more complex fracture sequence which generally involved the opening of a secondary crack in the

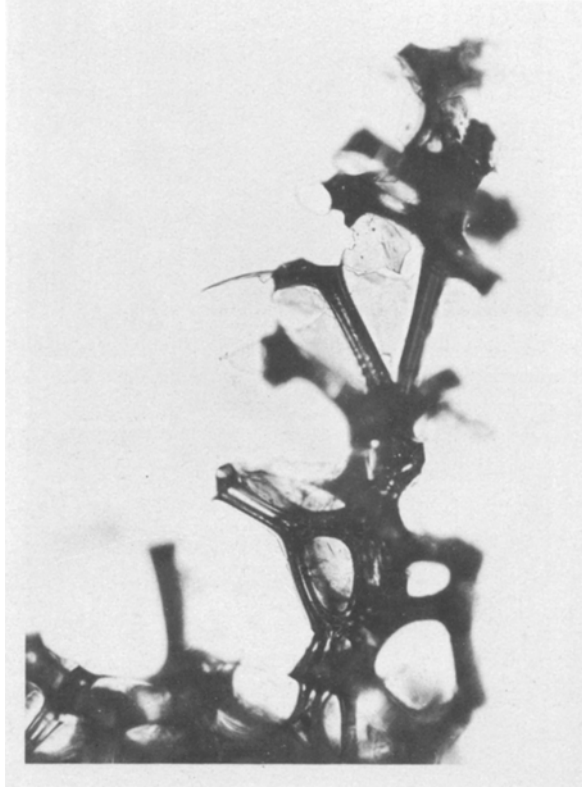

Figure 4 A typical pull-out fragment showing the broken struts radiating from the central composite strut.

TABLE I Comparison of tensile properties at test temperatures used

Foam	Ultimate tensile strength ($kN\ m^{-2}$)		Tensile modulus ($MN\ m^{-2}$)	
	20° C	−196° C	20° C	−196° C
Unreinforced	897	1476	19.1	51.6
(S.D.)	(30.6)	(69.0)	(3.2)	(7.8)
Reinforced (normal size concentration)	963	1425	27.4	76.5
(S.D.)	(32.0)	(155)	(12.4)	(7.6)
Reinforced (low size concentration)	1095	1917	34.0	95.5
(S.D.)	(50.2)	(192)	(3.2)	(20.3)

cells adjacent to the end of the bundle, reflecting a high stress concentration in this area. The secondary crack opened parallel to the main crack, as shown in Fig. 5, inducing a torsional moment in the intervening matrix material and precipitating failure.

Single glass filaments up to 12 mm long and carbon filaments up to 6 mm long acted as crack arrestors and diverters in the same way as the small bundles. Single filaments with lengths greater than these, fractured in the plane of the matrix crack without any debonding or pull-out. Fig. 6 shows the path of a crack that has passed through a filament without substantial diversion from its plane in the matrix.

Examination of the fractured test pieces from the $80\ kg\ m^{-3}$ foams showed the same pull-out features as did the lower density material.

Figure 5 Primary crack (I) arrested by a large bundle and secondary crack (II) opening at the bundle end.

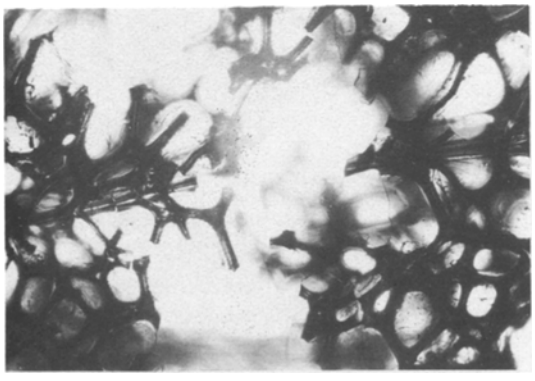

Figure 6 A single filament which has broken in the plane of the matrix crack without debonding.

3.3. Mechanical properties

Table I compares the tensile results obtained at both room temperature and −196° C for an unreinforced foam with those for two samples of the same foam reinforced with the same weight percent of chopped glass. There is no significant increase in strength in the first foam but the second foam, which was prepared with the fibre having the low size concentration, does show an increase. Both samples show an increase in modulus, the greater gain being exhibited by the second foam.

4. Discussion

Only in the case of a single filament was fibre fracture noted; a bundle always acted as a unit with no fracture or slippage within the bundle. It was found that glass fibres in large bundles are not effective as reinforcing agents in polyurethane foam; their presence gives rise to stress concentrations that weaken the structure. On the other hand, small bundles or individual filaments can arrest a crack and then divert it to give a longer fracture path and generate pull-out fragments. This indicates a potential toughening mechanism. The surface treatment of the fibres has no direct effect on the fracture properties of the composite, although it can affect the dispersion of the glass and the resultant bundle size.

The manner in which an array of cells builds up on a single filament is represented in Fig. 7a;

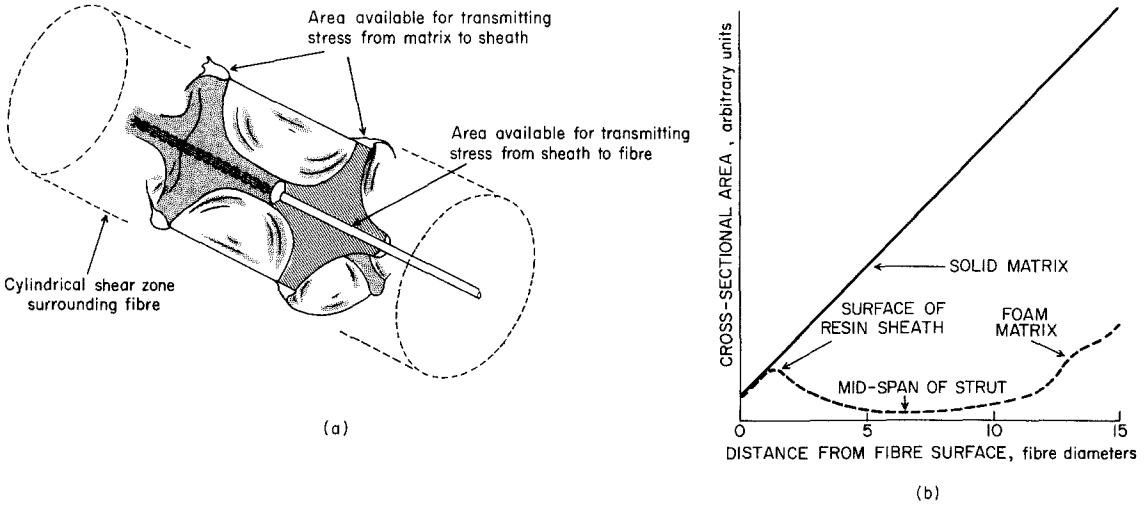

Figure 7 (a) Principal stress transfer zones for a single filament composite strut in polyurethane foam. (b) Comparison of stress transfer areas with increasing distance from fibre surface for a solid matrix composite and a polyurethane foam composite.

a similar arrangement may be visualized for a multi-filament core. An elongated composite strut is formed in which the filament is encased in a solid resin sheath. The interface between the glass and the resin is defined as the surface of a closed cylinder of essentially the same diameter as that of the filament, and the whole of the curved surface of the cylinder is available for transferring stress from the sheath to the filament [20]. However, the major portion of stress reaching the sheath from the matrix is channelled through the radial struts and the total cross-sectional area of solid material at the mid-span of the struts is much less than the surface area of the interface. This is the reverse of the situation in a composite with solid matrix, in which the surface area of a hypothetical cylinder about a fibre increases linearly with distance from the fibre surface as shown in Fig. 7b.

There are two principal stress transfer zones, one the classical interfacial region, and the other located in the cells adjacent to the fibre. An approximate value for the ratio of interface to strut areas can be derived by assuming a regular close packing of spherical cells about the core. For cells of radius R arranged with three cells in each plane and adjacent planes rotated 60° to obtain close packing, the inter-cell distance will equal $R\sqrt{3}$. The number of radial struts for a filament of length l, where $l \gg R$, is then $3l/R\sqrt{3}$.

The total cross-sectional area a of the struts of radius r is given by

$$a = \pi r^2 \cdot 3l/R\sqrt{3}.$$

Whereas the surface area of the filament a' of the same radius r is given by

$$a' = 2\pi rl.$$

The ratio of filament to strut areas becomes:

$$\frac{a}{a'} = \frac{2\pi rlR\sqrt{3}}{3l\pi r^2}.$$

As measurements have shown that R is of the order of $10r$ for the low-density foam the ratio of filament to strut area is 12:1.

Calculations of stress intensity about a crack tip in solid matrix composites predict that the interfacial bond should be about one fifth of the matrix cohesive strength for effective crack arrest. [21] Experimental studies have shown an even greater difference between these entities [22]. From the foregoing considerations of stress transfer zones, it would appear that a further reduction in bond strength by a factor of 12 would be necessary to prevent premature failure in the matrix. In the foams studied, however, elimination of all chemical bonding was insufficient to allow fibre debonding to occur on tensile fracture. The remaining source of strong bonding between fibre and resin sheath must be derived from physical bonding enhanced by shrinkage of the sheath around the fibre [23, 24].

The bulk ultimate tensile strength of the foams tested rarely exceeded 2 MN m^{-2}, with a shear

strength of about half that value. By way of comparison, the non-chemical or physical bonding between glass fibre and solid polyester resin is [25] of the order of 25 MN m^{-2}, and for Type I carbon fibres in epoxy resin it is reported [26] to be 15 MN m^{-2}. It seems unlikely, therefore, that a sufficiently weak interfacial bond can be created, and for all practical purposes the system must be regarded as matrix limited.

The energy absorbing mechanism in this system will be the work done in breaking the radial struts and in drawing the broken stubs through the bulk matrix as the crack opens. When a crack is deflected by a fibre it must follow a longer path, which implies an increase in fracture surface area and an increase in tensile strength [27].

When the fibres enter the pre-foamed mixture, they are in intimate contact with each other as in a normal composite. As the foam expands, the fibres (bundles or single filaments) tend to become separated from each other and to a large extent they become isolated within the matrix and there is a tendency for each reinforcing element to act independently of its neighbours. In considering critical length therefore, the model based on an isolated filament is not too far removed from the practical case.

In such a situation fracture will occur in the plane of the matrix crack when the ultimate tensile strength of the fibre/resin composite strut is exceeded by the shear strength of the foam matrix along its length. Thus it is possible to estimate the critical fibre length.

Considering a single filament in its sheath, the rule of mixtures gives:

$$\sigma_c = \sigma_f \cdot V_f + \sigma_s \cdot V_s.$$

The volume fraction terms can be replaced by the radii of the filament and sheath respectively:

$$\sigma_c = \sigma_f \cdot \pi r_f^2 + \sigma_s \cdot \pi (f_s^2 - r_f^2).$$

But $\sigma_s \ll \sigma_f$ and $r_s \gg 2r_f$; therefore, the contribution of the sheath toward the strength of the composite strut can be ignored.

$$\sigma_c = \sigma_f \cdot r_f^2.$$

The shear force acting on the surrounding cylinder of foam at break is:

$$\tau_c = \tau_m^{ult} \cdot \pi dl,$$

where d is the diameter of the outer stress transfer zone. When

$$\tau_c = \sigma_c, \tau_m^{ult} \cdot \pi dl = \sigma_f \cdot \pi r_f^2$$

$$l = \frac{2\sigma_f r_f^2}{\tau_m^{ult} d}.$$

The critical length is twice the above value, and for a matrix-limited system in which failure occurs in a region remote from the interface,

$$l_{cm} = \frac{2\sigma_f r_f^2}{\tau_m^{ult} d}.$$

where l_{cm} is the maximum fibre length for reinforcement of the foam.

From published data [28] it can be deduced that the load on a single 13 μm glass filament at failure in tension is about 0.3 N. The bulk shear strength, estimated from the measured tensile strength, indicates that the low-density foam (35 kg m^{-3}) used in the failure mechanism studies will have a shear force acting on the surrounding cylinder of foam at a distance of 6 filament diameters (where from observations the struts are thinnest) of around 0.05 N per mm length of filament. The critical filament length in this case would, therefore, be 2 x 0.3/0.05 = 12 mm. This is supported by the experimental work in which glass filaments of 12 mm and longer were seen to fracture in the plane of the matrix crack. Carbon fibres of 6 mm and longer and of similar aspect ratio as the glass filaments behaved in the same manner.

For higher foam densities, the shear strength increases, and a corresponding decrease in critical length will follow. Although it is not yet known whether the shear zone diameter d is also density dependent, by using the same value for d as in the low-density foam, a critical length for the 80 kg m^{-3} foam of 5 mm is predicted.

At some finite density, where the cell sizes have diminished and the relative strut thickness has increased, the proportion of solid material will raise the shear strength of the matrix to the level of the interfacial bond strength. At this point, which can be estimated to be at a density in excess of 500 kg m^{-3} for the particular foam formulation used, the critical length will be reduced to a fraction of a millimetre, and a system that embodies a high proportion of single filaments might be expected to approximate in its failure mechanisms to a solid matrix composite.

The fracture surfaces of the test pieces from

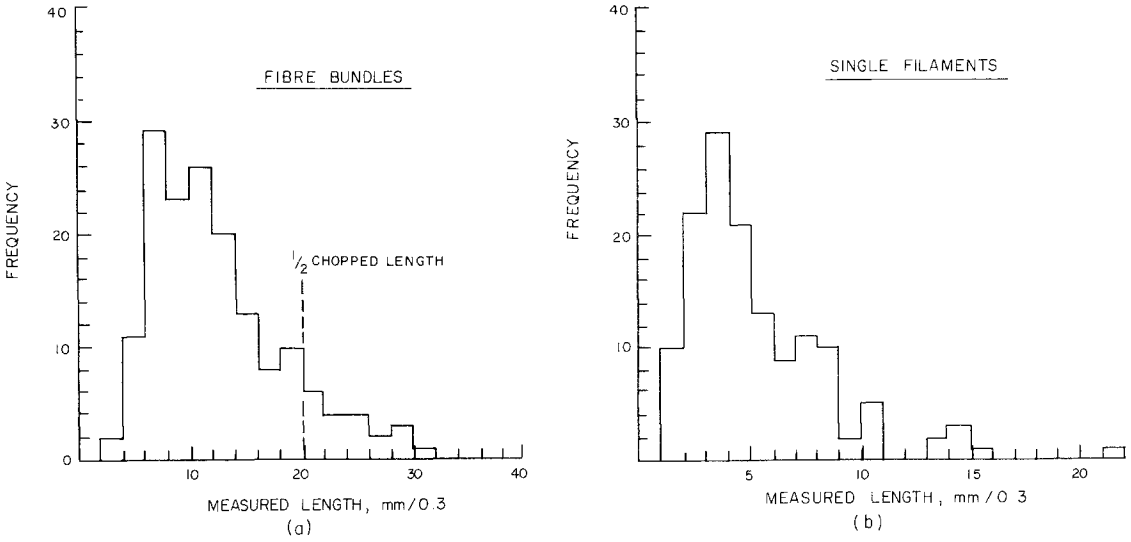

Figure 8 (a) Histogram of fibre bundle pull-out lengths measured directly from photomicrographs of fracture surfaces from tensile tests at room temperature. (b) Histogram of single filament pull-out lengths measured as in in (a).

the second reinforced foam supported populations of both fibre bundles and individual filaments. If each of the reinforcing elements had acted completely independently, it might be expected that in the case of the bundles, which could not break, there would be a rectangular distribution of all possible lengths up to half of the original chopped length visible on the surface. However, analysis of the pull-out lengths measured directly from photomicrographs of the surface shows that the distribution is not rectangular but approximates to a skewed normal distribution as shown in Fig. 8a. A histogram of the distribution of single filaments (Fig. 8b) gives the same type of distribution but with a much shorter cut-off.

The cut-off length for the bundles is far beyond the half chopped length (6 mm ≡ 20 mm on the histogram). An explanation for this, in part, can be assigned to the presence of some bundles which have failed to chop cleanly and are thus of twice the normal length. Most of the excessive protruding lengths are due to subsurface artefacts such as crossing fibres and the presence of skins which naturally occur in a sprayed-foam matrix. These locally strengthen the matrix, making it possible for the shorter portion of the fibre to remain in the matrix whilst the longer length is pulled from the corresponding face. Fig. 9. shows a section taken from a fracture surface with about two-thirds of a small 12 mm bundle protruding above the surface and the intersecting fibres below the surface restraining the shorter portion.

In the case of single filaments, there are very few in excess of 11 mm on the histogram in Fig. 8b. This corresponds to a 3.3 mm maximum pull-out length on the fracture surface. The longer lengths that are recorded may contain two or more filaments within the core but these appear as single filaments under the low magnification used. There is considerable difficulty in recognizing very short bundles and filaments, and this explains their low frequency of occurrence in both histograms.

Both the single filaments and the bundles were originally chopped to 12 mm, which is greater than the critical length predicted for a single filament by the model. If a crack approaches an isolated single filament at a point less than $\frac{1}{2}l_{cm}$ from one end, then pull-out would normally occur. If this shorter end is now anchored, then the filament will break since the longer portion cannot pull out. Therefore the maximum observed length of single filaments represents half the critical fibre length. The value thus derived, 6.6 mm, agrees reasonably well with the predicted value ot 5 mm.

Table I shows a consistent variation in the improvement in tensile properties of the two systems studied for both room temperature and −196°C measurements. This can be understood by an examination of the fracture morphology of the test specimens. The outstanding feature in

both cases is the presence of a considerable number of fibre bundles but the foam with the low size concentration also contains a high proportion of single filaments. The bundles of fibres with the higher concentration of size have remained much more closely bound than those in the second case where the foam has penetrated into the fibres to give a more open bundle. The appearance of the two types of bundle is contrasted in Fig. 10.

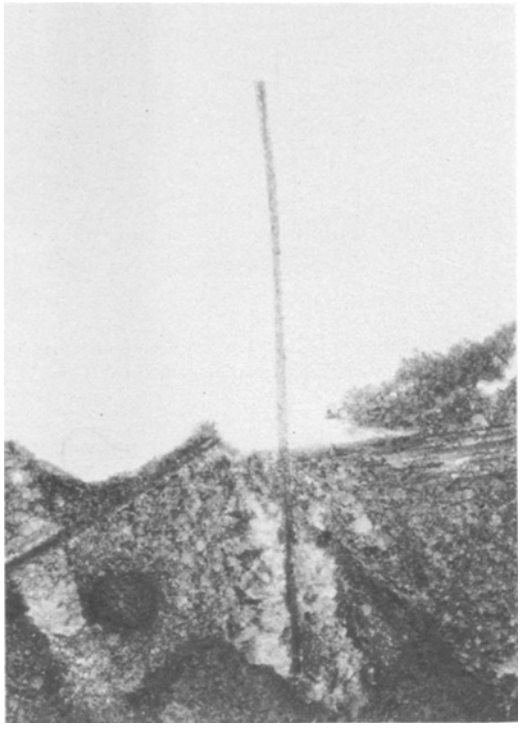

Figure 9 Section of tensile test specimen showing a long pull-out length with the shorter portion of the bundle anchored by intercepting fibres below the fracture surface.

The stress concentration at the end of the more closely bound bundle will create a tendency for a secondary crack to open, as in Fig. 5, which will weaken the structure. The more diffuse nature of the second bundle will give rise to a lesser stress concentration and the increased surface area generated by the fibre results in a net increase in tensile strength.

In both systems there is an increase in modulus; in the second case, the greater number of reinforcing elements forming composite struts results in a greater increase in modulus.

5. Conclusions

The presence of single filaments and small bundles in the rigid free-rise polyurethane foams studied causes localized changes in the foam morphology. This results in a matrix-limited system in which the interface assumes a passive role during tensile fracture irrespective of the surface treatment of the fibre and the test temperature. However, the surface treatment of glass fibres affects the degree of dispersion of the filaments and the resultant composite properties.

A critical fibre length is defined for these systems in which fracture occurs remote from the interface. It is dependent on the matrix shear strength which is in turn a function of foam density.

For the same glass content, greater increases in strength and modulus are obtained when a low

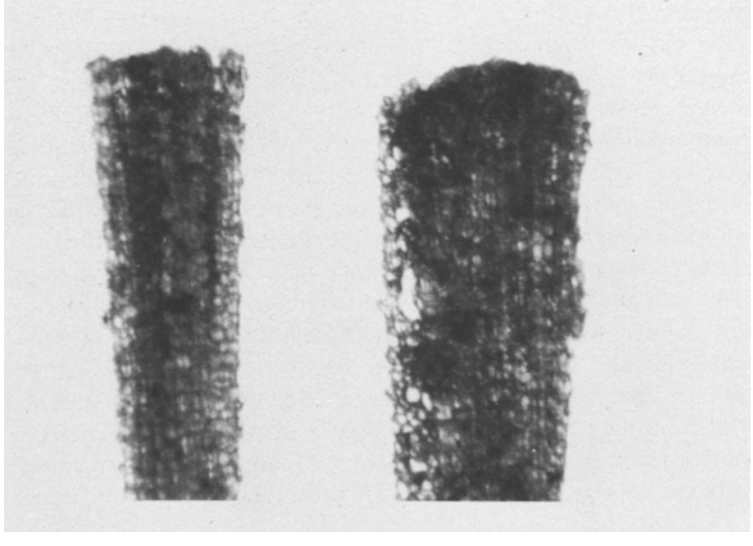

Figure 10 Comparison of pull-out fragments of fibre bundles with (left) 1 wt% surface treatment and (right) the lower concentration, 0.7 wt% which has allowed better penetration of the foam.

size concentration, which allows the bundles to form filaments is used.

References

1. K. C. FRISCH and J. H. SAUNDERS, eds., "Plastic foams", Parts 1 and 2 (Marcel Decker, New York, 1972 and 1973).
2. R. H. HARDIN, "Resinography of cellular plastics", edited by E. Blair, *ASTM publ.*, STP 414 (1967).
3. P. J. PHILLIPS and N. R. WATERMAN, *Polymer Eng. Sci.* **14** (1974) 67.
4. N. R. WATERMAN and P. J. PHILLIPS, *ibid* **14** (1974) 72.
5. T. E. NEET, *J. Cell. Plast.* Jan/Feb (1975) 45.
6. G. MENGES and F. KNIPSCHILD, *Polym. Eng. Sci.* **15** (1975) 623.
7. C. W. FOWLKES, *Int. J. Fracture* **10** (1974) 99.
8. W. BROY, J. NICHT and D. TREPTE, *Plaste. Kaut.* **21** (1974) 37.
9. V. P. CHERPANOV *et al., Sov. Plastics* **21** (1973) 6; Trans. ex *Plast. Massy.* **12** (1973) 9.
10. *Idem, Plast. Massy.* **5** (1974) 73.
11. *Idem, Int. J. Polymer Sci. Tech.* **2** (3) (1975) 4; Trans. ex *Plast. Massy.* **10** (1974) 60.
12. *Idem, ibid* **2** (9) (1975) 5; Trans. ex *Plast. Massy.* **1** (1975) 1.
13. G. KUEHNE and O. MERKER, *Plaste. Kaut.* **20** (1973) 39.
14. Anon, *Mod. Plast.* November (1969) 66.
15. P. MODIGLIANI, 25th Annual Technical Conference (1970), Reinf. plast/comps. div. SPI Inc. Sec. 8-C.
16. T. KAWANKA, *Jap. Plast. Age* July (1973) 24.
17. R. KLEINHOLZ and A. NEWMANN, *Kunstoffe* **64** (1974) 742.
18. Mitsubishi Chemical Industries Ltd, UK Pat. No. 1 438 226 (June 1976).
19. NASA, U.S. Pat. No. 3, 916, 060 (October, 1975).
20. H. L. COX, *Brit. J. Appl. Phys.* **3** (1952) 72.
21. J. COOK and J. E. GORDON, *Proc. Roy. Soc.* **A282** (1964) 508.
22. A. KELLY, *ibid* **A319** (1970) 95.
23. N. G. McCRUM, ed., "A review of the science of reinforced plastics" (HMSO, London, 1971) p. 85.
24. H. W. C. YIP and J. B. SHORTALL, *J. Adhesion* **7** (1976) 311.
25. J. B. SHORTALL and H. W. C. YIP, *Faraday Spec. Dis. Chem. Soc.* **2** (1972).
26. Courtaulds Ltd, "Graphil" data sheet.
27. R. H. KNIBBS, *J. Nuclear Mats.* **24** (1967) 174.
28. Fibreglass Ltd, FRP design data.

Received 21 July and accepted 27 July 1976.